Transient analysis of subcritical/ supercritical carbon dioxide based natural circulation loop with end heat exchangers: experimental study

Ajay Kumar Yadav, Maddali Ramgopal & Souvik Bhattacharyya

Heat and Mass Transfer
Wärme- und Stoffübertragung

ISSN 0947-7411

Heat Mass Transfer
DOI 10.1007/s00231-017-2038-z

Springer

Heat Mass Transfer
DOI 10.1007/s00231-017-2038-z

ORIGINAL

Transient analysis of subcritical/supercritical carbon dioxide based natural circulation loop with end heat exchangers: experimental study

Ajay Kumar Yadav[1] · Maddali Ramgopal[2] · Souvik Bhattacharyya[2]

Received: 3 August 2016 / Accepted: 3 April 2017

Abstract Carbon dioxide (CO_2) based natural circulation loops (NCLs) has gained attention due to its compactness with higher heat transfer rate. In the present study, experimental investigations have been carried out to capture the transient behaviour of a CO_2 based NCL operating under subcritical as well as supercritical conditions. Water is used as the external fluid in cold and hot heat exchangers. Results are obtained for various inlet temperatures (323–353 K) of water in the hot heat exchanger and a fixed inlet temperature (305 K) of cooling water in the cold heat exchanger. Effect of loop operating pressure (50–90 bar) on system performance is also investigated. Effect of loop tilt in two different planes (XY and YZ) is also studied in terms of transient as well as steady state behaviour of the loop. Results show that the time required to attain steady state decreases as operating pressure of the loop increases. It is also observed that the change in temperature of loop fluid (CO_2) across hot or cold heat exchanger decreases as operating pressure increases.

List of symbols

c_p	specific heat capacity(J/kgK)
Cu	Copper
D	internal diameter of inner pipe or loop diameter (m)
d_o	external diameter of inner pipe or loop diameter (m)
g	gravitational acceleration (m/s^2)
H_0	total height of vertical pipe (m)
L	length of CHX (sink) and HHX (source) (m)
L_0	total length of a horizontal pipe (m)
L_1	adiabatic pipe length on horizontal pipe (m)
m	mass flow rate (kg/s)
Q	heat transfer rate (W)
q''	heat flux (W/m^2)
R	Radius of curvature for bends (m)
SS	Stainless steel
T	temperature (K)
t	time (s)

Greek letters

ΔT	loop fluid temperature difference between riser and downcomer centres (K)
ΔT_w	temperature rise/drop of water across the CHX or HHX (K)

Subscripts

CHX	cold heat exchanger, sink
CO_2	carbon dioxide
HHX	hot heat exchanger, source
w	water

1 Introduction

Natural circulation loops (NCLs) are attractive due to their simplicity and reliability. In recent years, there has been an increasing interest towards the application of carbon dioxide in the area of cooling, heating and power generations. Revival of CO_2 as a refrigerant in the recent past was reviewed by Pearson [1]. Carbon dioxide based NCLs are very compact in comparison to other conventional working fluids due to the

✉ Ajay Kumar Yadav
ajaykyadav@nitk.edu.in

[1] Department of Mechanical Engineering, National Institute of Technology Karnataka, Surathkal 575025, India

[2] Department of Mechanical Engineering, Indian Institute of Technology Kharagpur, Kharagpur, WB 721302, India

Published online: 10 April 2017

favourable thermophysical properties of CO_2 [2, 3]. CO_2 based NCLs have been proposed for several heat transfer applications such as new generation nuclear reactors [4], chemical extraction [5, 6], cryogenic refrigeration [7], heat pump [8], electronic cooling systems [9], geothermal [10, 11], and solar thermal applications [12]. However, detailed studies on CO_2 based NCLs are limited in literature. Yanagisawa et al. [13] carried out experimental studies on a two-phase NCL that employed CO_2 as secondary fluid in a vapour compression refrigeration system that used ammonia as primary refrigerant. Kumar and Ramgopal [14] carried out experimental study on a CO_2 loop with end heat exchanger in subcritical region (vapour phase, liquid phase and liquid and vapour phases) by varying the amount of CO_2 charged into the loop as well as the external fluid temperatures. Chen et al. [15] carried out an experimental investigation on steady state performance of a CO_2 based thermosyphon operating near critical point. They observed small change in bulk mean temperature across the cooler near to pseudocritical points in supercritical region. Manish et al. [16] conducted experiments in a supercritical pressure natural circulation loop (SPNCL) with carbon dioxide as working fluid. They used electric heater in place of HHX and observed instability in a narrow window of power with the loop operating in the pseudo-critical temperature range. Liu et al. [17, 18] carried out experimental study in a simple rectangular loop with vertically placed heating section to study the steady-state characteristics of supercritical CO_2 based NCL. They investigated the effects of system pressure, inlet temperature, heat flux, and buoyancy force on the system behaviour. No instabilities in the flow were observed during the experiment. Archana et al. [19] carried out experiment to study the transient behavior of supercritical CO_2 based NCL with electric heater in place of HHX, and developed one-dimensional transient code. Swapnalee et al. [20] reported test results for supercritical CO_2 and water based NCLs. They considered a heater at the bottom and cold heat exchanger at the top, and presented results for steady state only.

Experimental studies on NCLs employing supercritical CO_2 with end heat exchangers are rarely reported in the open literature [14, 21], and the same is true for experiments on transient analysis of supercritical CO_2 based NCLs. To fill in that critical void, this study presents experimental studies of subcritical/supercritical CO_2 based NCL with end heat exchangers. Results are presented on the transient behaviour of the loop at various operating pressures and temperatures. Loop transient behaviour has been studied for various tilt angles as well in XY and YZ planes. The operating parameter range is chosen such that the loop fluid (CO_2) exists as a subcritical or supercritical single-phase fluid. This experimental work will make it easier for future researchers to validate their numerical models and carry out more parametric studies to understand the loop behaviour.

2 Experimental facility and procedures

2.1 Experimental facility

A detailed schematic of the test facility employed in this study is shown in Fig. 1a. The arrangement comprises two tube-in-tube heat exchangers (hot heat exchanger and cold heat exchanger) and two vertical tubes (riser and downcomer). Additionally, a CO_2 reservoir (expansion tank) is also employed in the test rig.

Both the heat exchangers are counter flow tube-in-tube type; CO_2 flows in the inner tube while the external fluid (water) flows in the outer annulus. K-type thermocouples (11 sensors, range: −270 °C to 1260 °C, accuracy: 0.4%) of suitable length are attached to measure CO_2 and water side temperatures (positions of temperature sensors are shown in Fig. 1a). Two RTDs (Type: Pt100, range: −100 °C to +200 °C) are also employed to measure the temperature of CO_2 at the centre of left and right legs.

The 15L CO_2 reservoir, employed to function as an expansion tank, was kept in a water bath. This is required to maintain loop at a constant operating pressure.

Figure 2 shows a photographic view of the test facility. A thermostatic bath (Julabo Model F25, range: −20 °C to +150 °C, accuracy: ± 0.01 °C) having a heating capacity of 2 kW is used to supply constant temperature water to the hot heat exchanger. A chilled water circulator (Julabo model F1701, range: −40 °C to +40 °C, accuracy: ± 0.1 °C) of 1 kW capacity (at 273 K) is used to supply chilled water at constant temperature to the cold heat exchanger. To measure the mass flow rate of water, two calibrated rotameters (0–10 LPM range, least count: 0.1 LPM) are connected separately to both the external fluid systems and mass flow rate of water is controlled by valves.

A Bourdon pressure gauge (0–200 bar, least count: 5 bar) is connected at the centre of left leg. Thermocouples are attached to the outside surface of SS tubes by aluminium tape. Thermocouples used for measuring water inlet and outlet temperature from the heat exchangers are in direct contact with water. Two RTDs monitored the temperature of CO_2 at the centre of left and right legs. Sensors of both the RTDs are fitted in direct contact with the internal loop fluid CO_2. A computer integrated data acquisition system (Yokogawa, Model MW100, accuracy: ± 0.01 °C) is employed to collect and store various temperature data of the loop. Geometric details of the test rig are given in Table 1. The setup is designed such that the loop can be

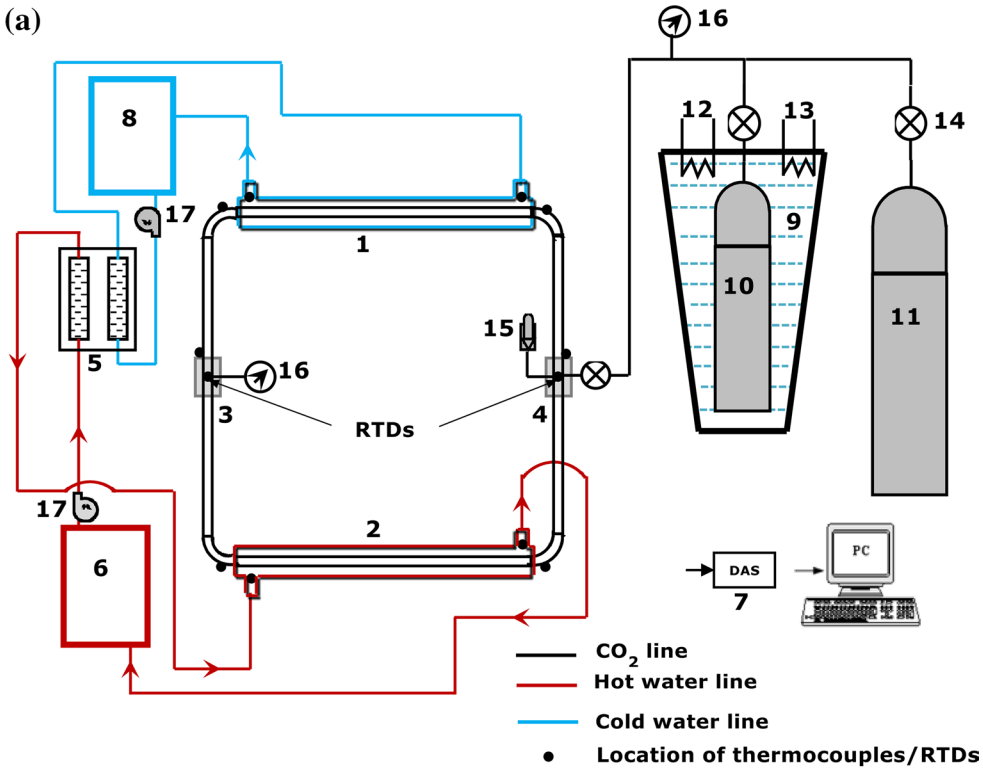

1: CHX, 2: HHX, 3: Left leg (Riser), 4: Right leg (downcomer), 5: Rotameters, 6: Thermostatic bath for HHX, 7: Data acquisition system, 8: Thermostatic bath for CHX, 9: Water bath for expansion tank, 10: CO_2 reservoir cylinder (expansion tank), 11: CO_2 cylinder, 12: Heating coil, 13: Cooling coil, 14: Valve, 15: Safety valve (pressure relief valve), 16: Pressure gauge, 17: Water pump

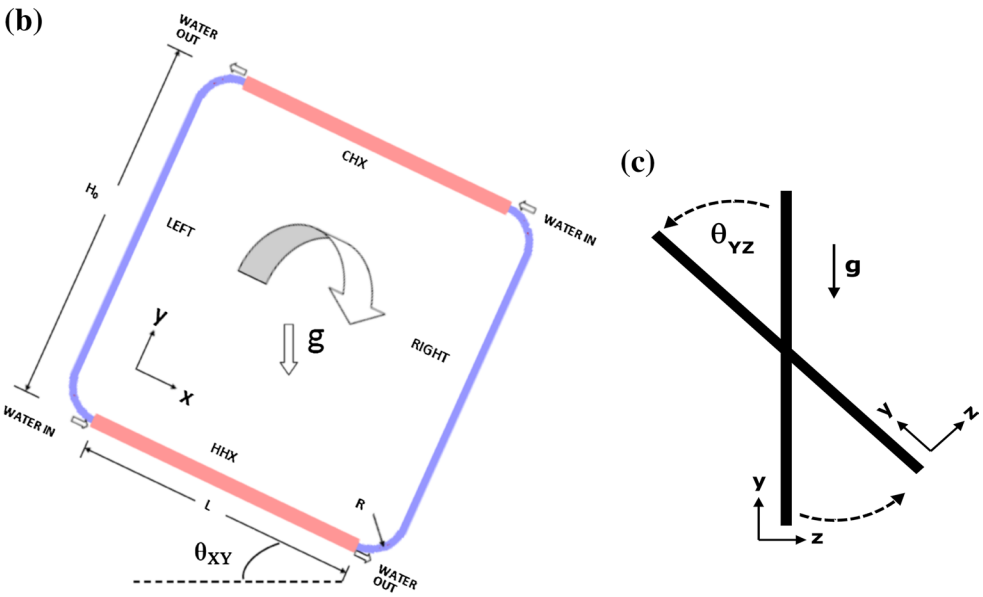

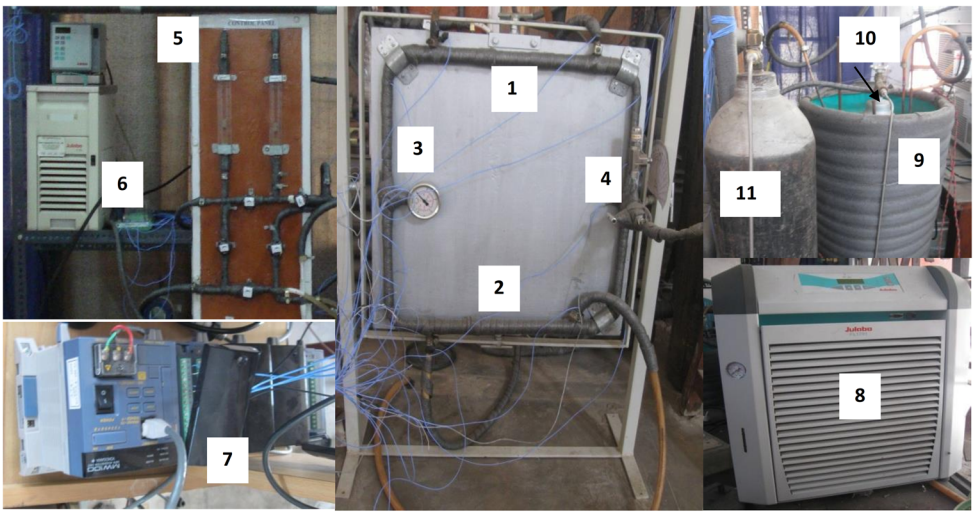

Fig. 2 Photographic view of the test facility

1: CHX, 2: HHX, 3: Left leg (Riser), 4: Right leg (downcomer), 5: Rotameters, 6: Thermostatic bath for HHX, 7: Data acquisition system, 8: Thermostatic bath for CHX, 9: water bath for expansion tank, 10: CO_2 reservoir cylinder (expansion tank), 11: CO_2 cylinder.

Table 1 Geometric details of experimental setup

Parameters	Values
HHX and CHX:	
Inner tube inner diameter (SS)	7.3 mm
Inner tube outer diameter (SS)	9.6 mm
Outer tube inner diameter (Cu)	16 mm
Outer tube outer diameter (Cu)	19.2 mm
Total Length including side wall thickness (Cu)	400 mm
Internal length (Cu)	390 mm
Height of riser/downcomer	500 mm
Internal diameter of riser/downcomer	7.3 mm
Height of riser/downcomer	500 mm
Radius of curvature at bends	50 mm
Material of the loop	SS
Volume of expansion tank	15 L

Table 2 Range of operating variables for subcritical/supercritical phase during experiment

Parameters	Range	Error range (%)
System pressure	50–90 bar	±2.5
Hot water inlet temperature (T_H)	323–353 K	±0.315
Cold water inlet temperature (T_C)	305 K	±0.315
Cold water flow rate (m_{wc})	0.0167–0.05 kg/s	±10
Hot water flow rate (m_{wh})	0.0167–0.05 kg/s	±10

tilted at any required angle in XY or YZ plane as illustrated in Fig. 1b, c.

2.2 Experimental procedure

Before starting the experiment for transient analysis, initial temperature of the loop was maintained uniform at 305 K by circulating water in CHX and HHX at required temperature. To achieve higher operating pressure (in the case when CO_2 cylinder pressure is lower), loop fluid is precooled up to the calculated temperature (using equation of state for CO_2) at cylinder pressure. Thereafter, water at 305 K was circulated in CHX and HHX to achieve the initial condition. Excess pressure, if any, is relieved to CO_2 cylinder. The entire range of operating variables is presented in Table 2 as a test matrix. All temperatures are recorded at an interval of 0.5 s. Each test run is carried out from the initial state to steady state and steady state to stop/final state. Steady state condition is assumed to be reached based on the temperature reading satisfying the standard steady-state norms at any location of the loop. The expansion tank is maintained at the operating pressure of the loop, and it is connected at the centre of right insulated leg of the loop.

3 Results and discussion

Unless otherwise mentioned, the mass flow rate of water in CHX as well as in HHX is maintained constant at a value of 0.05 kg/s. From calculations it is seen that this flow rate ensures turbulent flow on the water side. Initial

loop temperature is maintained at 305 K before the start of experiment. It may be noted that most of the transient analysis results have been plotted for a position at the centre of left leg.

3.1 Effect of pressure

Influence of system operating pressure on the transient behaviour of the loop has been studied experimentally for a fixed water inlet temperature of CHX (305 K) and HHX (323 K). Figure 3 shows the variation of CO_2 temperature at the left leg centre for different operating pressures. Results indicate that the system reaches steady state quickly when the operating pressure is high. It may be attributed to good thermo physical properties of fluid at higher pressure. At constant temperature, all thermo physical properties (i.e., density, specific heat, volumetric expansion coefficient, viscosity) of CO_2 increase with increase in operating pressure. A higher value of these thermo physical properties except viscosity is favourable for NCLs and these properties in combination lead the system to reach steady state faster. Table 3 depicts the approximate time to reach steady state for different operating pressure. It can be seen that there is an abrupt drop in time to reach steady state as operating pressure changes from 60 to 70 bar. This occurs due to the additional effect of operating a loop near critical/pseudocritical condition at which thermo physical properties are most favourable to NCL. It is worth mentioning here that the critical pressure and temperature of CO_2 are 73.8 bar and 304.3 K. In the present study, average operating temperature (314 K) of the loop lies near the pseudocritical point (313.1 K) for 90 bar which causes the system to reach steady state faster at 90 bar.

Table 3 Time to reach steady state for different operating pressure

Pressure (bar)	50	60	70	80	90
Time (s)	950	850	350	300	170

3.2 Effect of tilt

Experiments are carried out to study the effect of loop tilt angle on loop behaviour. The loop is tilted in XY plane as well as in YZ plane. Figure 4 shows the variation of loop fluid (CO_2) temperature at the centre of the left leg with time for different angles of tilt and at an operating pressure of 90 bar. Results show that the time taken to reach steady state is almost the same in all the cases at 90 bar. Experiments are also conducted for other pressures and same trend is observed. Effect of tilt on temperature of loop fluid (at left leg centre) can be seen clearly at 45° tilt angle. As loop is tilted in YZ plane, effective height of the loop decreases which reduces the buoyancy effect and causes temperature of the loop to increase. At a tilt angle of 30°, there is no significant change in temperature of loop fluid compared to 0° tilt angle. This is also observed in a numerical study carried out by Yadav et al. [22]. Lower loop temperature is observed in the case of tilting loop by 45° in XY plane. It occurs due to more stable (unidirectional) flow compared to tilting in YZ plane or 0° case [22, 23].

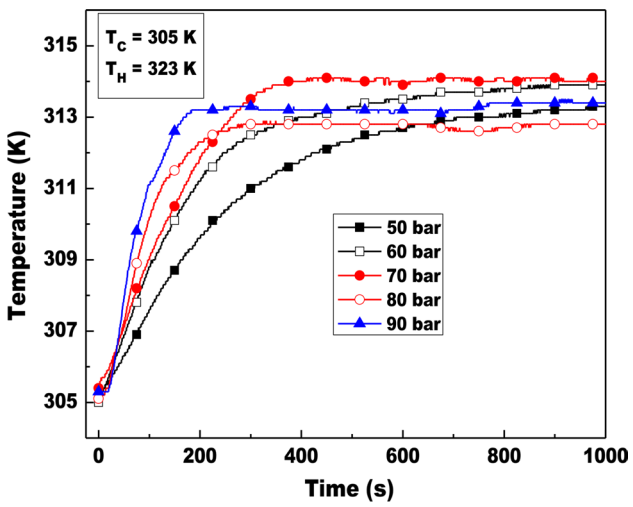

Fig. 3 Variation of loop fluid (CO_2) temperature at left leg centre with time for different operating pressure

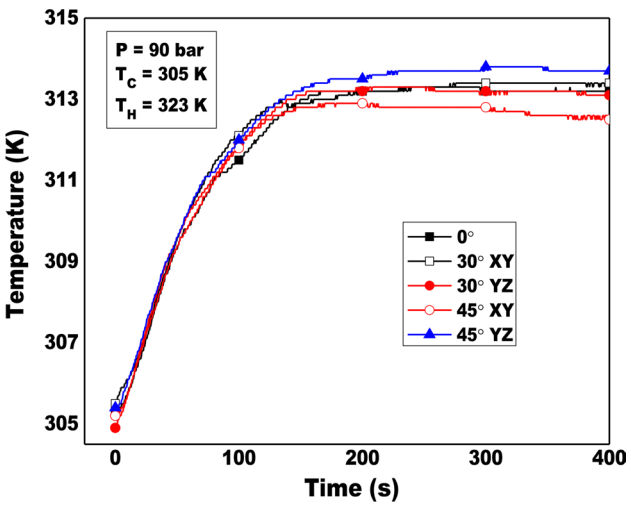

Fig. 4 Variation of loop fluid (CO_2) temperature at left leg centre with time for different angles of tilt at 90 bar

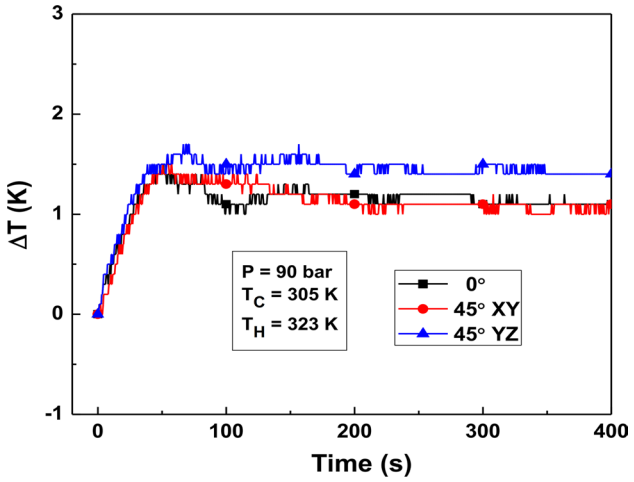

Fig. 5 Variation of the loop fluid (CO_2) temperature difference for different tilt angles

3.3 Effect of tilt on temperature difference between riser and downcomer

Test results on the temperature difference between riser and downcomer are obtained at 90 bar for different angles of tilt and are shown in Fig. 5. The loop is tilted in XY plane as well as in YZ plane. At a higher angle of tilt (45°)in the YZ plane, mass flow rate of loop fluid decreases due to weaker buoyancy effect [21, 22] leading to an increase in temperature difference between the left leg and the right leg. Whereas, in the case of tilt in XY plane, temperature difference between left and right leg is less due to more stable (unidirectional) flow as explained above in Sect. 3.2.

3.4 System behaviour under changing hot water inlet temperature for different pressures

Figure 6 depicts system behaviour under changing hot water inlet temperature (323–353 K) at an operating pressure of 90 bar. Initially hot water inlet temperature is set at 323 K. After the loop fluid (CO_2) attains steady state and the system is allowed to function for a few more minutes in this condition, warm water inlet temperature is increased step wise (10 K per step) up to 353 K. This leads to a similar step escalation in heat transfer rate. Similar results (transient behaviour of the loop) are observed for other operating pressures (50–80 bar). Figure 7 shows the effect of operating pressure and hot water inlet temperature on the loop fluid temperature difference between left leg centre and right leg centre. It is observed that as pressure increases, the temperature drop or rise of loop fluid decreases. This effect could be attributed to favourable thermophysical properties of CO_2 at higher pressures near critical or pseudocritical point. From simulation results [24–27] it is evident that near the critical or pseudocritical point, Reynolds number is very high which indicates high mass flow rate as well as high heat transfer rate. Specific heat capacity near critical/pseudocritical region reaches the maximum which also leads to a fall in temperature difference.

Unlike the previously reported experimental studies [2], where constant heat flux was applied at the heat source, the present investigation with heat exchangers at both ends, exhibits no oscillations or pulsating flow within the range of study.

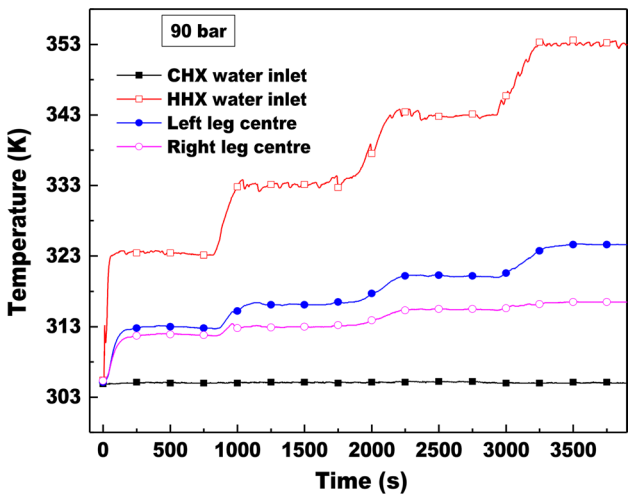

Fig. 6 Temperature variation with time under varying hot water inlet temperature at 90 bar

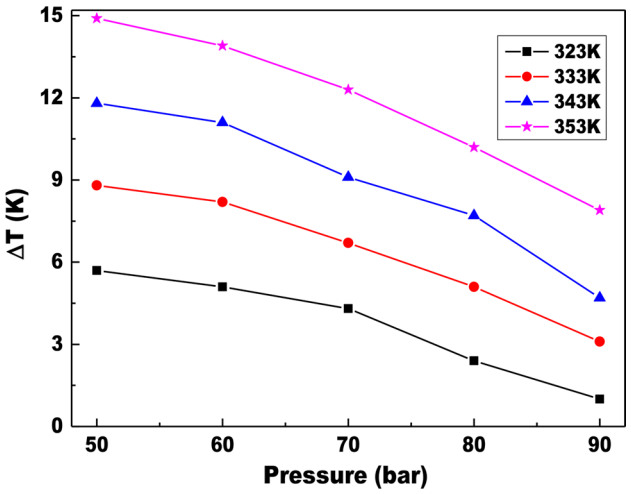

Fig. 7 Effect of operating pressure on loop fluid temperature at different hot water inlet temperatures

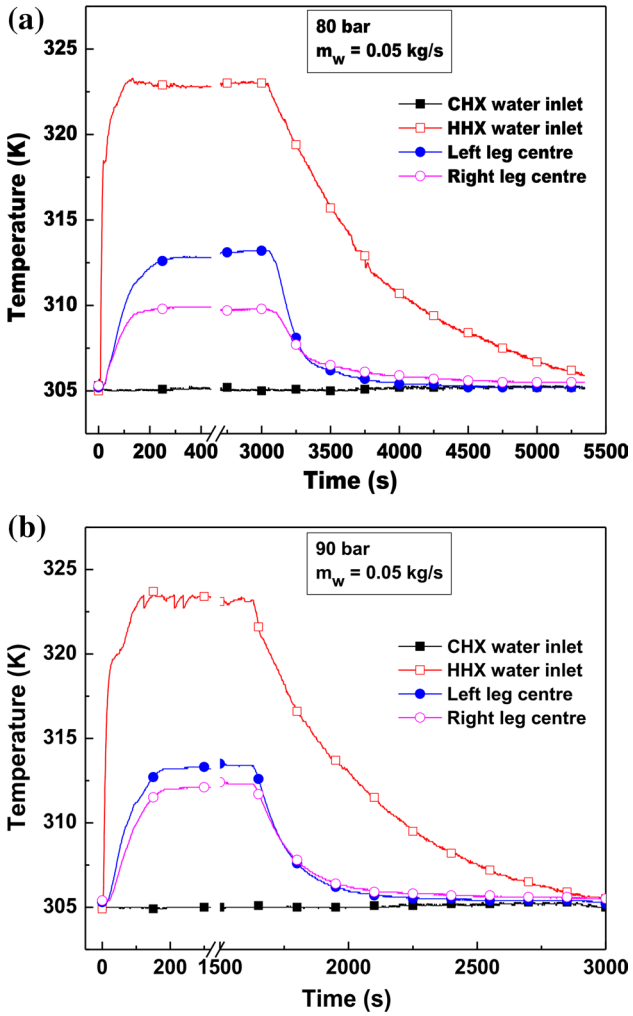

Fig. 8 Die down time of system at operating pressure of **a** 80 bar and **b** 90 bar

3.5 Effect of pressure on die down (pull down) time

Figure 8a, b shows the time taken to reach the initial state from steady state at 80 and 90 bar respectively. The test protocol for this particular exercise required the hot water circulating pump to be switched off after the system reached steady state and then the system was allowed to cool down keeping cold water pump in running condition. Results were obtained for a hot water inlet temperature of 323 K, which was maintained before switch OFF. Time taken to reach initial state to steady state and vice versa is higher at 80 bar (300 and 2200 s) than that at 90 bar (170 and 1400 s). This occurs due to the excellent thermophysical properties (higher specific heat and higher volumetric expansion coefficient) of the fluid at higher pressure (90 bar). It may be inferred that the system should be operated near critical/pseudocritical region to obtain faster response. Results also show that the loop is stable and no oscillating or pulsating flow is observed in the present range of study.

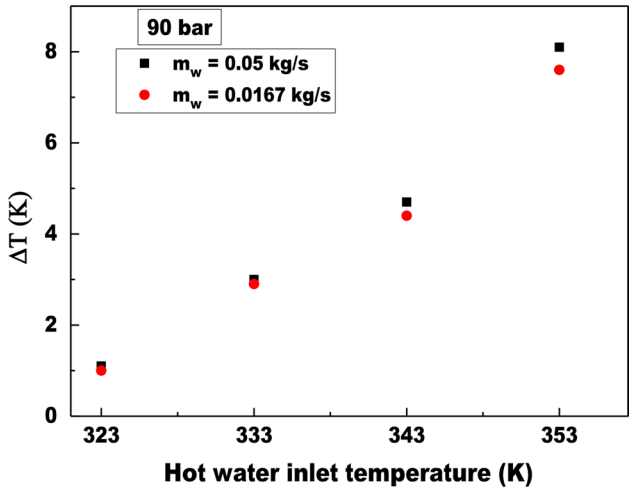

Fig. 9 Effect of hot water inlet temperature and water mass flow rate at operating pressure of 90 bar

3.6 Effect of water inlet temperature and mass flow rate

Figure 9 shows the effect of water inlet temperature and mass flow rate on the loop fluid temperature difference (ΔT) between left leg and right leg. Water mass flow rate at both the heat exchangers are kept the same. Hot water inlet temperature of HHX is varied from 323 to 353 K while keeping the cold water inlet temperature of CHX constant at 305 K. Results show that at higher water mass flow rate (i.e., high Reynolds no.) in CHX/HHX, temperature difference of loop fluid is higher in all the cases. It occurs due to higher heat transfer coefficient at water side in the heat exchangers. Results also show the increase in loop fluid temperature difference as water inlet temperature of HHX increases. It occurs due to higher buoyancy effect caused by larger temperature difference between CHX and HHX.

3.7 Variation of temperature with time at different locations

Variation of temperature with time at different locations of the loop is presented in Fig. 10 at a system pressure of 90 bar. Even though the system is insulated, a temperature difference of 0.5 K is observed between bottom and top of the riser (left leg). This temperature difference may be attributed to pressure drop of CO_2 as well as the heat loss to the ambient due to imperfections in the insulation employed. Similarly small temperature difference (0.3 K) is observed between the downcomer (right leg) top and bottom as well. Figure 10 also shows the temperature drop/

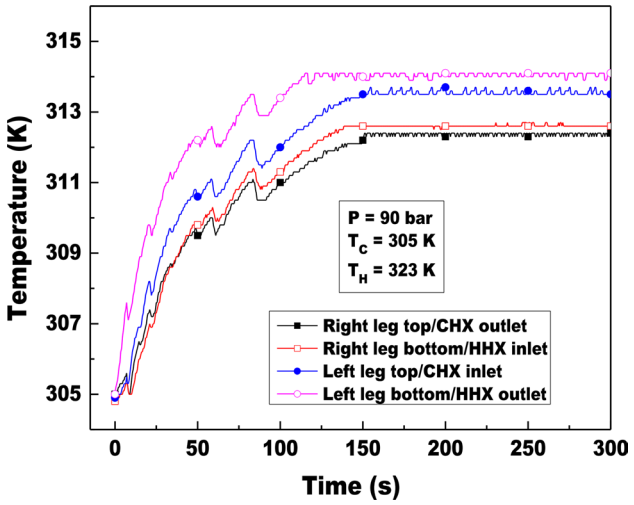

Fig. 10 Variation of loop fluid (CO_2) temperature with time at different locations

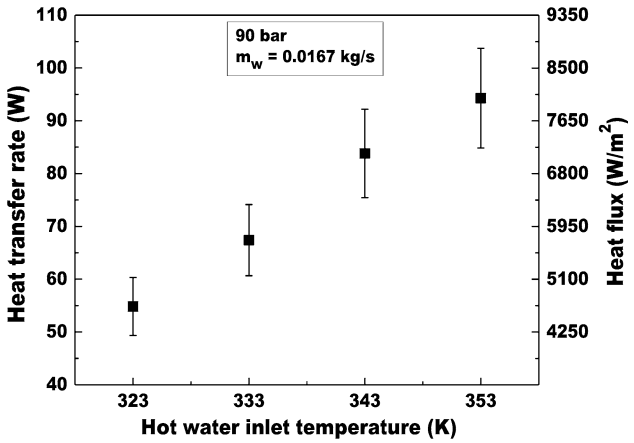

Fig. 11 Variation of heat transfer rate and heat flux at varying hot water inlet temperatures at 90 bar

rise of CO_2 across HHX and CHX. Temperature drop/rise in both the heat exchangers is not exactly the same due to a greater heat loss in the HHX than the CHX.

3.8 Variation of heat transfer rate and heat flux with temperature of HHX

From experiments, heat transfer rate is estimated based on the change in water temperature at CHX or HHX for an operating pressure of 90 bar. Figure 11 shows the variation of heat transfer rate as well as heat flux at varying hot water inlet temperatures. A low mass flow rate of water (0.0167 kg/s) is maintained to obtain measurable temperature difference of water across the heat exchanger, as this will lead to smaller error in the measurement of temperature difference. An average of more than 100 steady state results was considered to calculate the water temperature difference across the heat exchanger. Results shows that as HHX water inlet temperature increases, the heat transfer rate as well as heat flux increase due to higher buoyancy effect caused by temperature difference.

Heat transfer rate (Q) is calculated using water inlet and outlet temperature at HHX or CHX.

$$Q = m_w c_{p,w} \Delta T_w \tag{1}$$

where, m_w is mass flow rate of water, $c_{p,w}$ is specific heat of water and ΔT_w is water temperature difference between inlet and outlet of the heat exchanger.

Heat flux (q'') is given by,

$$q'' = \frac{Q}{\pi d_o L} \tag{2}$$

Where, d_o is the outer diameter of the internal loop, and L is the length of heat exchanger.

3.9 Uncertainty analysis

Uncertainty analysis is carried out to appropriately capture the measurement errors in the results presented.

Functional dependency of the various performance parameters (specific heat of water is assumed to be constant), given as:

$$Q = f(\dot{m}_w,\ \Delta T_w) \tag{3}$$

Heat transfer rate (Q) is calculated by considering the following parameters:

Minimum mass flow rate measured is 1.0 LPM and least count is 0.1 LPM. Hence maximum uncertainty in case of mass flow rate measurement is.

$$\frac{\Delta m_w}{m_w} = \frac{0.1}{1} = \pm 0.1 = \pm 10\% \tag{4}$$

Minimum temperature measured is 32 °C and least count is 0.1 °C. Hence, the maximum uncertainty in case of temperature measurement with data acquisition system is.

$$\frac{\Delta T_w}{T} = \frac{0.1}{32} = \pm 0.003125 = \pm 0.3125\% \tag{5}$$

Uncertainty in calculating heat transfer rate is.

$$\frac{\Delta Q}{Q} = \left[\left(\frac{\Delta m_w}{m}\right)^2 + 2\left(\frac{\Delta T_w}{T}\right)^2\right]^{1/2} \tag{6}$$

$$\frac{\Delta Q}{Q} = \left[(0.1)^2 + 2(0.003125)^2\right]^{1/2} = 0.10 = 10\%$$

The error bar in the form of uncertainty in calculating heat transfer rate is shown in Fig. 11.

4 Conclusions

Experimental investigations have been carried out to study the transient and steady state behaviour of a CO_2 based NCL. Subcritical and supercritical phases of the CO_2 are considered with an operating pressure in the range of 50–90 bar and an operating temperature range of 323–353 K. Conclusions from the test results can be enumerated as:

1. Results show that the time required for reaching steady state decreases as operating pressure of the loop increase. There is an abrupt drop in time to reach steady state as operating pressure approaches to critical/pseudocritical condition.
2. Temperature of loop fluid (at left leg centre) at a tilt angle of 45° in YZ plane is higher compared to tilt in XY plane due to reduction in effective height of the loop. At a tilt angle of 30°, there is no significant change in temperature of loop fluid compared to 0° tilt angle.
3. Effect of tilt in XY plane as well as in YZ plane on the time to reach steady state is not found to be significant within the range of study.
4. As operating pressure increases, the temperature difference between riser and downcomer decreases due to higher specific heat capacity and volumetric expansion coefficient at higher pressures.
5. As HHX water inlet temperature increases, the heat transfer rate as well as heat flux increase due to higher buoyancy effect caused by temperature difference.
6. At higher water mass flow rate, temperature difference of loop fluid across the CHX or HHX is higher due to high heat transfer rate at heat exchangers.
7. Within the range of study (50–90 bar, 323–353 K), the NCL is found to be stable.

Acknowledgment The study has been carried out under a project sponsored by Extramural Research Division, Council of Scientific and Industrial Research (CSIR), Government of India. The financial support provided by CSIR is gratefully acknowledged.

Compliance with ethical standards

Conflict of interest On behalf of all authors, the corresponding author states that there is no conflict of interest.

References

1. Pearson A (2005) Carbon dioxide—new uses for old refrigerant. Int J Refrig 28:1140–1148
2. Kumar KK, Ramgopal M (2009) Carbon dioxide as secondary fluid in natural circulation loops. Proc IMechE, Part E: J Process Mech Eng 223:189–194
3. Yadav AK, Ramgopal M, Bhattacharyya S (2012) CO_2 based natural circulation loops: new correlations for friction and heat transfer. Int J Heat Mass Transf 55:4621–4630
4. Dostal V, Hejzlar P, Driscoll MJ (2006) The supercritical carbon dioxide power cycle: comparison to other advanced power cycles. Nucl Technol 154:283–301
5. Bondioli P, Mariani C, Mossa E, Fedelli A, Muller A (1992) Lampante olive oil refining with supercritical carbon dioxide. J Am Oil Chem Soc 69:477–480
6. Fourie FCVN, Schwarz CE, Knoetze JH (2008) Phase equilibria of alcohols in supercritical fluids Part I. The effect of the position of the hydroxyl group for linear C8 alcohols in supercritical carbon dioxide. J Supercrit Fluids 47:161–167
7. Yamaguchi H, Zhang XR, Fujima K (2008) Basic study on new cryogenic refrigeration using CO_2 solid–gas two phase flow. Int J Refrig 31:404–410
8. Ochsner K (2008) Carbon dioxide heat pipe in conjunction with a ground source heat pump (GSHP). Appl Therm Eng 28:2077–2082
9. Kim DE, Kim MH, Cha JE, Kim SO (2008) Numerical investigation on thermal–hydraulic performance of new printed circuit heat exchanger model. Nucl Eng Des 238:3269–3276
10. Kreitlow DB, Reistad GM (1978) Themosyphon models for down hole heat exchanger application in shallow geothermal systems. J Heat Transf 100:713–719
11. Torrance KE (1979) Open-loop thermosyphons with geological application. J Heat Transf 100:677–683
12. Chen L, Zhang X (2014) Experimental analysis on a novel solar collector system achieved by supercritical CO_2 natural convection. Energy Convers Manag 77:173–182
13. Yanagisawa Y, Fukuta M, Ogura N, Kaneo H, Operating characteristics of natural circulating CO_2 secondary loop refrigeration system working with NH_3 primary loop. In: Proceedings of the 6th IIR-Gustav Lorentzen Natural Working Fluids Conference, 2004
14. Kiran Kumar K, Ramgopal M (2011) Experimental studies on CO_2 based single and two-phase natural circulation loops. Appl Therm Eng 31:3437–3443
15. Chen L, Deng BL, Zhang XR (2013) Experimental investigation of CO_2 thermosyphon flow and heat transfer in the supercritical region. Int J Heat Mass Transf 64:202–211
16. Sharma M, Vijayan PK, Pilkhwal DS, Asako Y (2013) Steady state and stability characteristics of natural circulation loops operating with carbon dioxide at supercritical pressures for open and closed loop boundary conditions. Nucl Eng Des 265:737–754
17. Liu G, Huang Y, Wang J, Lv F, Leung LHK (2016) Experiments on the basic behavior of supercritical CO_2 natural circulation. Nucl Eng Des 300:376–383
18. Liu G, Huang Y, Wang J, Leung LHK (2016) Heat transfer of supercritical carbon dioxide flowing in a rectangular circulation loop. Appl Therm Eng 98:39–48
19. Archana V, Vaidya AM, Vijayan PK (2015) Flow transients in supercritical CO_2 natural circulation loop. Proc Eng 127:1189–1196
20. Swapnalee BT, Vijayan PK, Sharma M, Pilkhwal DS (2012) Steady state flow and static instability of supercritical natural circulation loops. Nucl Eng Des 245:99–112
21. Kiran Kumar K, Ramgopal M (2009) Steady-state analysis of CO_2 based natural circulation loops with end heat exchangers. Appl Therm Eng 29:1893–1903
22. Yadav AK, Ramgopal M, Bhattacharyya S (2014) Transient analysis of subcritical/supercritical carbon dioxide based natural circulation loops with end heat exchangers: numerical studies. Int J Heat Mass Transf 79:24–33
23. Yadav AK, Ramgopal M, Bhattacharyya S (2016) Effect of tilt angle on subcritical/supercritical carbon dioxide based natural

circulation loop with isothermal source and sink. ASME J Therm Sci Eng Appl 8:011007-1–011007-8
24. Sabersky RH, Hauptmann EG (1967) Forced convection heat transfer to carbon dioxide near the critical point. Int J Heat Mass Transf 10:1499–1508
25. Yadav AK, Bhattacharyya S, Ramgopal M (2016) Optimum operating conditions for subcritical/supercritical fluid based natural circulation loops. ASME J Heat Transf 138:112501-1–112501-9
26. He S, Kim WS, Jackson JD (2008) A computational study of convective heat transfer to carbon dioxide at a pressure just above the critical value. Appl Therm Eng 28:1662–1675
27. Yadav AK, Ramgopal M, Bhattacharyya S (2012) CFD analysis of a CO_2 based natural circulation loop with end heat exchangers. Appl Therm Eng 36:288–295